Activation of Invariant Natural Killer T Cells Further Ameliorates Post-Infarct Cardiac Remodeling in Mice With MSC Transplantation

Wentao Li
Zhengzhou University People's Hospital https://orcid.org/0000-0003-4896-1479
YI HUANG
Zhengzhou University People's Hospital
CHUANYU GAO (gaocy6804@163.com)
Zhengzhou University People's Hospital https://orcid.org/0000-0001-5153-1205
ZHONGYU ZHU
Zhengzhou University People's Hospital
GUOYOU DAI
Zhengzhou University People's Hospital

Research article

Keywords: bone marrow mesenchymal stem cells, invariant natural killer T cells, myocardial infarction

Posted Date: May 20th, 2021

DOI: https://doi.org/10.21203/rs.3.rs-520311/v1

Abstract

Background

The purpose of this study was to examine the effect of MSCs on the infiltration of iNKT cells and further observe whether the activation of iNKT cells could assist the therapeutic action of MSCs on ventricular remodeling.

Methods

Mice with MI were sacrificed at day 7, 14, 28 and hearts were excised. qRT-PCR for Vα14Jα18 (a special marker of iNKT cell for C57BL/6) was carried out. 25μL serum-free medium(Me)□complete medium with 1×106 MSCs or without MSCs were respectively injected into myocardium in five points. After 7, 14, 28 days, qRT-PCR for Vα14Jα18 was respectively preformed. Gene expressions of Vα14Jα18 in PLV with the injection of cMe alone and cMe with PGE2, L-NMMA, indomethacin, anti-TGF at day 7 were also analyzed. Then, the experiment was performed in five groups: MI+Me, MI+MSCs, MI+MSCs+indome, MI+α-GC and MI+MSCs+ α-GC. After 28 days, heart tissue fibrosis was accessed by Masson trichrome dyeing and apoptosis was evaluated by TUNEL staining and western blotting for caspase-3 protein.

Results

The iNKT cells infiltrating into the PLV was significantly increased at day 7 after MI (1.72-fold changes from baseline, P<0.05), but almost returned to baseline level at day 14 and 28. Compared to MI+Me group(1.76±0.20-fold), iNKT cells infiltration was significantly suppressed at day 7 in MI+MSCs (1.25±0.29-fold, P<0.05) and MI+cMe groups (1.19±0.25-fold, P<0.05). In MI+cMe+indome and MI+cMe+PGE2 group, the changes of iNKT cells infiltration were respectively 1.74- and 1.04-fold (vs 1.20-fold in MI+cMe group, P<0.05). Combined MSCs transplantation with iNKT cells activation, myocyte apoptosis and interstitial fibrosis in PLV were both significantly attenuated.

Conclusions:

In the infarcted mouse model, MSCs suppressed the infiltration of iNKT cells by secreting PGE2. Activating iNKT cells could assist the therapeutic effect of MSCs on ventricular remodeling, with attenuated apoptosis and interstitial fibrosis.

Background

With acute occlusion of the coronary artery, a shortage of oxygen and nutrients is present in the heart during myocardial infarction (MI), which leads to necrosis and apoptosis. Acute myocardial infarction and heart failure, which often follow, are major causes of death and disability worldwide. New therapies are required to limit myocardial infarct size, to prevent adverse left ventricular remodeling, and to reduce the onset of heart failure following MI (1). All of these factors trigger a strong inflammatory reaction, resulting in a highly inflammatory environment in the post-MI heart (2,3). The balance between

inflammatory and reparative phases is subtle and requires proper fine-tuning to prevent excessive inflammation or inadequate stimulation of repair (4). The inflammatory response to MI plays a critical role in determining MI size. A persistent proinflammatory reaction can contribute to adverse postinfarction remodeling; ultimately, excessive inflammation results in limited capacity for self-renewal and adverse remodeling, which finally leads to depressed left ventricular (LV) function (5). All of these factors make inflammation an important therapeutic target for improving outcomes following AMI.

Administration of mesenchymal stem cells (MSCs) in an animal model of MI yields variable degrees of functional improvement and is a promising tool for the treatment of a range of human degenerative and inflammatory diseases. MSCs are applied as a form of regenerative medicine, mainly based on their capacity to differentiate into specific cell types and to act as bioreactors of soluble factors that promote tissue regeneration (6). In addition to these regenerative properties, the discovery that MSCs hold an immunoregulatory capacity was made over a decade ago, when it was observed that MSCs abrogated T-cell proliferation *in vitro* (7). The immune system has a critical role in the pathogenesis and progression of a number of degenerative diseases, raising the possibility that MSCs may be effective in repairing damaged organs by promoting cell formation and modulating the associated immune response. Based on this premise, the immunogenicity and immunomodulatory properties of MSCs have been thoroughly characterized to evaluate their potential clinical application (8-11). MSCs were reported to interact with several cell types of the immune system and may be an excellent means to reduce detrimental inflammatory reactions (12).

As the regulation of the inflammatory reaction appears to be inefficient after massive necrosis, the interest of current research has turned towards the induction of anti-inflammatory or regulatory subsets of immune cells to reduce apoptosis and fibrosis. Invariant natural killer T (iNKT or type 1 NKT) cells are innate-like T lymphocytes that coexpress αβT-cell receptor and NK cell markers and recognize glycolipid antigens (13). Moreover, iNKT cells have a protective role against autoimmune and neoplastic diseases, including acute liver injury (14) and rheumatic disease (15). As reported by Sobirin *et al.* (16) and Homma *et al.* (17), activation of iNKT cells by α-galactosylceramide (α-GC), a specific activator of iNKT cells (18), ameliorates myocardial ischemia/reperfusion injury and postinfarct cardiac remodeling in mice.

In 2009, Prigione *et al.* (8) demonstrated that human bone marrow MSCs abolished the proliferation and interferon (IFN)-γ production of iNKT cells *in vitro* through the release of soluble factors. While the effects of MSCs on iNKT cells appear to be ideal in an *in vitro* scenario, inflammation *in vivo* is complex, which may have unpredictable influences on MSCs, and further exploration and validation with an animal model for the interaction between MSCs and iNKT cells are required. If *in vivo* MSCs inhibit the infiltration of iNKT cells in the postinfarction heart, we wondered whether activating iNKT cells before MSC transplantation can have a synergistic effect on LV remodeling. The present study aims to demonstrate the effect of MSCs on iNKT cells *in vivo* and to investigate further the potential therapeutic value of MSC transplantation together with iNKT cell activation on LV remodeling.

Methods

Animals. All experiments were performed in accordance with the ethics code for animal experimentation. Ethical approval for all work was received from the animal research committee of Zhengzhou University (Zhengzhou, China). A total of 400 male C57BL/6J mice were purchased from Beijing HFK Bioscience Co., Ltd. (Beijing, China). The specific criteria for animal euthanasia included absence of food or water intake, low or no mobility, weak or absent heartbeat and absence of respiratory movement during the ongoing study, and all animals were euthanized at the end of the study. The mice were divided into different groups by sortition randomization method to control the cofounding bias. After intraperitoneal anesthesia (ketamine/midazolam 75 mg/kg and 5 mg/kg, respectively), mice were euthanized by cervical dislocation to minimize suffering. The method to confirm the death of mice included the absence of movement and heartbeat. All efforts were made to minimize suffering, including gaseous anesthesia with isoflurane (2-3%). Animals at 6-8 weeks of age (weight 20-25 g) were used for the experiments. Mice were kept in a pathogen-free environment at an invariable temperature and under a 12-h light-dark cycle. Pathogen-free chow and water sterilized using a high-pressure steam sterilizer were provided *ad libitum*.

MSC culture and expansion. MSCs isolated from the bone marrow of C57BL/6 mice were obtained from Cyagen Biosciences Inc. (Guangzhou, China). The identification of cells according to multipotency and the cell surface phenotypes was performed by the provider. The cell surface phenotypes were $CD29^+$, $CD44^+$, $Sca\text{-}1^+$, $CD117^-$ and $CD31^-$, characterized by fluorescence-activated cell sorting analysis（Fig.1）. The cells had the potential for differentiation into the osteogenic and adipogenic lineages as determined by staining with Alizarin red and oil red O, respectively. This evidence verified their identity as MSCs.

The mouse MSCs were cultured in Dulbecco's modified Eagle's medium supplemented with 10% fetal bovine serum (Gibco, Thermo Fisher Scientific, Inc., Waltham, MA, USA), penicillin (100 U/ml), streptomycin (100 mg/ml) and 2 mM L-glutamine at 37°C in a humidified atmosphere containing 5% CO_2. To obtain MSC clones, cells at 80-90% confluence were harvested and seeded into T25 flasks at $2x10^4$ cells/cm^2. Each clone was then picked and expanded. Cells at the 8^{th} to 10^{th} passages cultured in serum-free medium were used in the experiments.

Myocardial infarction and MSC transplantation. Mice were anesthetized by intraperitoneal injection of ketamine/medazolam (75 mg/kg and 5 mg/kg, respectively). With the application of a rodent ventilator, tracheal intubation was performed on the mice, a small thoracotomy was performed, and left anterior descending coronary artery (LAD) ligation was created as previously described (19), with a slight modification. A 10/0 Prolene suture was passed under the LAD at 1-1.5 mm distal to the left atrial appendage, immediately following the bifurcation of the major left coronary artery. At 1 h after surgical intervention, a total of $1x10^6$ C57BL6/J MSCs in 25 μl complete medium were injected into five different points of the peri-infarct LV region in the MI group or the LV region in the sham group (20). Five points were separately injected with $2x10^5$ MSCs in 5 μl medium. After 7, 14 and 28 days, TTC staining was performed to determine the infarct area of the LV. The remaining area of the LV was confirmed as the peri-infarct LV.

Experimental design

RT-qPCR for iNKT cells in post-MI hearts.

A total of 18 MI and 6 sham mice were created as described above. To observe time-dependent changes in iNKT cells, mice were sacrificed at 7, 14, and 28 days, and the LVs of their hearts were excised for reverse transcription-quantitative polymerase chain reaction (RT-qPCR) analysis. As in a previous study (21), RT-qPCR for Vα14Jα18 (a specific marker of iNKT cells in C57BL/6 mice) was performed.

RT-qPCR for iNKT cells in post-MI hearts with MSC transplantation.

At 1 h after surgery, MI and sham mice were randomly assigned to one of the following groups: i) 25 µl serum-free medium (Me) alone, ii) 25 µl complete cell-free medium after cell culture (cMe), or iii) 25 µl complete medium with $1x10^6$ MSCs injected into the myocardium of LV, with the suspension infused within 30 sec (22). Thus, there were six groups: Sham+Me (n=6), Sham+MSCs (n=6), Sham+cMe (n=6), MI+Me (n=18), MI+MSCs (n=18) and MI+cMe (n=18). After 7, 14 or 28 days, RT-qPCR analysis was performed to observe time-dependent changes in iNKT cells in the PLV area of the MI groups compared with those in the LV area of the sham groups.

To address the effective factors of cMe on the immunoregulation of MSCs, specific antagonists were used in the MI+cMe group: 20 µg/ml N^G-monomethyl-L-arginine (Sigma-Aldrich; Merck KGaA, Darmstadt, Germany), an inhibitor of inducible nitric oxide (NO) synthase (iNOS), 5 µM indomethacin (indome; ApexBio, Glendale, CA, USA) for inhibition of prostaglandin E_2 (PGE_2), or 10 µg/ml anti-transforming growth factor (TGF)-β1 monoclonal antibody (R&D Systems Inc., Minneapolis, MN, USA), according to a previous study (8). In the fourth group, prostaglandin E_2 (PGE_2) was added to the MI+cMe groups. Each group included 6 mice. Subsequently, after 7 days, RT-qPCR analysis of Vα14Jα18 was performed (20).

RT-qPCR for iNKT cells, Masson staining and TUNEL staining in post-MI hearts with MSC treatment and iNKT cell activation.

Mice were randomly divided into five groups. At 1 h after MI, one group was injected with serum-free medium (Me) as a control, and another two groups randomly received an injection of $1x10^6$ MSCs in 25 µl cMe with or without indome. In the fourth and fifth groups, α-galactosylceramide (α-GC; 0.1 µg/g body weight; Avanti Polar Lipids, Inc., Alabaster, AL, USA) was administered 30 minutes before MI specifically to activate iNKT cells while $1x10^6$ MSCs with 25 µl complete medium were also injected into the sixth group. Therefore, there were six groups: Sham+Me (n=6), MI+Me (n=15), MI+MSCs (n=18), MI+MSCs+indome (n=18), MI+α-GC (n=18) and MI+MSCs+α-GC (n=18). After 7 and 28 days, RT-qPCR analysis of Vα14Jα18 was performed. After 28 days, the mice were euthanized, and the hearts were obtained. Tissue fibrosis of the LV was assessed by Masson's trichrome staining, and apoptosis was evaluated by terminal deoxynucleotidyl transferase deoxyuridine triphosphate nick end labeling (TUNEL) and western blotting analysis for cleaved caspase-3 protein. Fibrotic and total areas of each image were measured by computerized planimetry (Image ProPlus 5.0, Media Cybernetics, Silver Spring, MD, USA), and the percentage of the fibrotic area was calculated as follows: (Fibrotic area/total area) x100%.

Methods of western blotting and TUNEL

Western blot analysis. Total protein was extracted from LV samples using IP lysis buffer after pulverizing in liquid nitrogen. The concentration of the protein was quantitatively measured by a BCA protein kit (Pierce, USA). The protein was mixed with loading buffer and boiled at 100°C for 10 min to denature it. Total protein (20 μg) was separated by 12% SDS-PAGE and transferred to 0.45 μm polyvinylidene fluoride (PVDF) membranes. After blocking with 5% nonfat-dried milk at room temperature for 1 h, membranes were incubated with primary antibodies [anti-cleaved caspase-3 antibody (Cat. No. ab49822; Abcam; USA) and anti-GAPDH antibody (Cat. ab181602 Abcam; USA)] overnight at 4°C and then incubated with horseradish peroxide-conjugated secondary antibodies at room temperature for 1 h. The blots were developed with ECL reagent (Millipore, Germany). GAPDH was used for normalization. The sum density of each protein band was measured by ImageJ software.

TUNEL. The mouse heart LV samples were dehydrated by standard graded alcohol solutions and embedded in paraffin as described previously (PMID: 31419728). LV samples in paraffin were sectioned longitudinally into 5 μm thin sections. After three washes with PBS (pH = 7.4), the sections were incubated with proteinase K for 30 min at 37°C. After treatment with cell permeable fluid (Servicebio, G1204), the sections were assayed using an *in situ* death detection kit (Roche, 11684817910) according to the manufacturer's instructions. All of the sections were counterstained with 4',6-diamidino-2-phenylindole (DAPI). Finally, the numbers of total cells and TUNEL-positive cells were counted in at least three noncontinuous fields of each specimen using an inverted fluorescence microscope (Zeiss, Germany). The percentage of positive cells (positive cells/total cells ×100) was determined as the apoptotic rate (%). Cell counting was performed by a pathologist blinded to the experimental conditions.

Statistical analysis. Data analysis was performed using SPSS software 18.0 for Windows (SPSS, Inc., Chicago, IL, USA). Values are expressed as the mean ± standard deviation. Each experiment was performed at least three times independently. Analysis of variance and ANOVA were performed for multiple and two-group comparisons. $P<0.05$ was considered to indicate a significant difference.

Results

Elevation of iNKT cell receptors in post-MI hearts.

The quantification of iNKT cells was verified by gene expression of cell surface receptor-Vα14Jα18 (Fig. 2). Similar to those in a previous study (16), the results indicated that the infiltration of iNKT cells into the peri-infarct LV (PLV) significantly increased at 7 days after MI (1.72-fold change vs. sham group; $P < 0.05$) but almost returned to baseline levels at 14 and 28 days after MI. A persistent elevation of Vα14Jα18 gene expression was observed in the infarct LV (ILV) at 7, 14 and 28 days after MI (1.79-, 1.77- and 1.72-fold change vs. sham group, respectively; $P < 0.05$).

Suppressive effect of MSCs on iNKT cells in the post-MI heart.

As presented in Fig. 3a, the values are all presented as the ratio of the Sham + Me group. RT-qPCR demonstrated that the gene expression of Vα14Jα18 was significantly suppressed at day 7 in the MI + MSCs (1.25 ± 0.29) and MI + cMe groups (1.19 ± 0.25) compared with the MI + Me group (1.76 ± 0.20; $P < 0.05$). However, the gene expression of Vα14Jα18 at day 7 in the MI + MSCs and MI + cMe groups was still higher than that in the corresponding sham groups (1.25 vs. 1.00; 1.19 vs. 1.01; $P > 0.05$), while the difference between the two treated groups was not significant. In addition, there was no significant difference between the MI + Me, MI + MSCs and MI + cMe groups at days 14 and 28.

Although the mechanisms of immunoregulation of MSCs are unknown, direct cell-to-cell contact and/or soluble factors, such as TGF-β1, NO and PGE_2, may mediate the effect. The results may indicate that soluble factors in complete medium after MSCs are cultured may have a major role in immunoregulation. The effect of the administration of antagonists and neutralizing antibodies of certain soluble factors on the gene expression of Vα14Jα18 was measured, and the results are shown in Fig. 3b. The specific inhibition of iNOS and TGF-β1 had no significant influence on the infiltration of iNKT cells, while a significant effect was observed with indome, a specific antagonist of PGE_2. As presented in Fig. 3b, in the MI + cMe + indome group, the quantified expression of Vα14Jα18 was 0.54-fold higher than that in the MI + cMe group (1.74- vs. 1.20-fold change; $P < 0.05$). To verify further the effect of PGE_2, 25 μl complete medium with added PGE_2 was injected into post-MI mice. The results indicated that the gene expression of Vα14Jα18 was obviously suppressed, with a significant difference compared with the MI + cMe + indome group (1.04- vs. 1.74-fold change; $P < 0.05$).

Synergistic effect of iNKT cells and MSC transplantation on ventricular remodeling

In mice treated with soluble factors and MSCs, quantification of Vα14Jα18 was performed at days 7 and 28 after MI, with values expressed as the fold-change of the Sham + Me group (Fig. 4). As indome is an antagonist of PGE_2, counteracting the effect of PGE_2, a significant difference between the MI + MSCs and MI + MSCs + indome groups was observed after 7 days (1.74- vs. 1.19-fold; $P < 0.05$) but not at 28 days. In the MI + α-GC and MI + MSCs + α-GC groups, the gene expression of Vα14Jα18 was significantly elevated in the PLV at day 7; however, it remained significantly increased at day 28 (6.7- vs. 2.6-fold in the MI + MSCs + α-GC group, 7.1- vs 2.7-fold in the MI + α-GC group), which was in accordance with the result of previous study (16), the gene expression of Vα14Jα18 in the MI + MSCs + α-GC group tended to be less than in the MI + α-GC group, but with no significant difference.

As presented in Fig. 5A, MI-associated apoptosis was significantly attenuated in the MI + MSCs group compared with that in the MI + Me group, and this effect was enhanced in the MI + α-GC and MI + MSCs + α-GC groups. There was no significant difference between the percentage of TUNEL-positive cardiomyocytes in the MI + MSC and MI + MSCs + indome groups, while a significant difference was found between the MI + α-GC and MI + MSCs + α-GC groups. The quantitative results for total TUNEL-positive cells in different regions of all groups were [the MI + MSCs + α-GC group (21.09 ± 5.23%) vs. the MI + α-GC group (31.02 ± 2.21%), $P < 0.05$; vs. the MI + MSCs + indome group (34.14 ± 5.87%), $P < 0.05$; vs.

the MI + MSC group (31.26 ± 5.3%), P < 0.05; vs. the MI + Me group (44.47 ± 6.09%), P < 0.05; the MI + MSCs + indome group (34.14 ± 5.87%) vs. the MI + MSC group (31.26 ± 5.3%), P > 0.05 Fig. 5a].

To investigate the underlying molecular mechanisms of the antiapoptotic effects of α-GC injection, the protein expression of caspase-3 in PLV heart tissue was analyzed by western blot analysis. The results indicated that the proapoptotic cleaved protein, caspase-3, was significantly attenuated in the MI + MSC group compared with the MI + Me group. Compared with the MI + MSC group, the level of caspase-3 was not significantly different in the MI + MSCs + indome and MI + α-GC groups, while it was significantly decreased in the MI + MSCs + α-GC group (Fig. 5b).

To observe the effect of MSCs on cardiac fibrosis, the fibrotic areas in the PLV and ILV sections were quantified. The PLV and ILV sections of MSC-treated hearts exhibited less fibrosis than those of Me-treated hearts (P < 0.05; Fig. 5c; Table 1). The MI + MSCs + indome group did not exhibit a significant difference in fibrotic area compared with the MI + MSC group, while compared with the MI + MSC and MI + α-GC groups, α-GC + MSCs significantly attenuated fibrosis (P < 0.05; Fig. 5c; Table 1).

Table 1
collagen volume fraction in 5 groups of mice()

	MI + Me (n = 4)	MI + MSCs (n = 5)	MI + MSCs +indome (n = 6)	MI + α-GC (n = 6)	MI + MSCs +α-GC (n = 6)
Infarct areas %	87.04 ± 1.37†	70.04± 1.34*†	68.02 ± 1.51*†	59.65 ± 1.97*†	51.68 ± 1.33*
Peri-infarct areas,%	20.70 ± 1.43†	16.60± 1.39*†	15.53 ± 1.47*†	13.23 ± 1.15*†	10.22 ± 0.79*
*P < 0.05 versus MI + Me; †P < 0.05 versus MI + MSCs + α-GC					

Discussion

The results of the present study demonstrated that MSC transplantation suppressed the infiltration of iNKT cells in the peri-infarct areas of C57BL/6 mice and that PGE_2 secreted by MSCs was involved. Previous studies have demonstrated the protective effect of iNKT cells on the postinfarct heart (16–17). In the present study, activation of iNKT cells by α-GC before MSC transplantation further ameliorated ILV and PLV remodeling after MI in mice, accompanied by decreases in interstitial fibrosis and apoptosis. The present study provided direct evidence for the suppressive effects of MSCs on iNKT cells *in vivo* and that iNKT cell activation further improved the efficacy of MSCs in the treatment of post-MI hearts.

MI causes sterile inflammation, which is characterized by the recruitment and activation of immune cells of the innate and adaptive immune systems. The tasks of these inflammatory cells, including neutrophils,

macrophages and lymphocytes, involve clearance of dead tissues, the reparative response and adverse remodeling (23–27). However, excessive chronic inflammation in the peri-infarct heart may cause further cell apoptosis and myocardial fibrosis, finally leading to impairment of cardiac function (28). The results of the present study are consistent with those of a previous study (16) in terms of iNKT cells (Vα14Jα18) infiltrating into the heart after MI. Previous studies have demonstrated that anti-inflammatory therapy attenuates LV dilation and contractile dysfunction, which are associated with a decrease in white blood cell infiltration (29, 30). Chronic inflammation in the post-MI heart, particularly in peri-infarct areas, has a crucial role in cardiac remodeling and failure after MI, while the precise role of inflammatory cells and chemokines in this process remains to be fully elucidated. Furthermore, iNKT cells rapidly mediate various functions by producing a mixture of T helper type 1 (TH1) and TH2 cell cytokines and a vast array of chemokines (13). Thus, iNKT cells may function as a bridge between the innate and adaptive immune systems and orchestrate tissue inflammation. Sobirin *et al.* (16) first demonstrated the increased infiltration of iNKT cells in post-MI hearts. A similar result was obtained in the present study.

Emerging evidence suggests that progenitor cells have immunomodulatory properties and specifically suppress the proliferation or activation of T cells (31). MSCs are considered to be one of the most promising progenitor cell types for therapeutic applications. In addition, MSCs have an immunoregulatory capacity and elicit immunosuppressive effects in various settings. These cells have immense plasticity coupled with their ability to modulate the activity of immune cells (12). Previous studies have indicated that *in vitro*-expanded MSCs exert broad-spectrum immunoregulatory functions on innate immune cells, including dendritic cells, NK cells and adaptive immune cells (10, 31). Prigione *et al.* (8) previously demonstrated that MSCs expanded from human bone marrow abolished the *in vitro* proliferation of resting peripheral blood $V\alpha24^{+}V\beta11^{+}$ cells through the release of PGE_2. The present study demonstrated that MSCs had a suppressive effect on iNKT cells in postinfarct mouse hearts by releasing PGE_2, with a reduction in iNKT cell infiltration in peri-infarct areas, which may be unbeneficial or even harmful. While previous studies (32–34) concluded that certain other molecules released by MSCs might be involved in the modulation of T cells, the results of the present study indicated that iNOS and TGF-β1 did not have any role in this modulation.

In the present study, the inhibitory effect of MSCs on iNKT cells was abolished by the nonselective cyclooxygenase inhibitor indomethacin, which is an inhibitor of PGE_2, while α-GC, which is well known to activate iNKT cells (35), significantly increased the infiltration of iNKT cells in the peri-infarct area. The iNKT cell-surface receptors, including T-cell receptor (TCR) and NK1.1, become downregulated following MI, which renders iNKT cells invisible by flow cytometric detection (36, 37). The downregulation of TCR remains until at least 24 h; subsequently, iNKT cells rapidly proliferate and increase to the peak level at 72 h after α-GC administration (36–40). The present study demonstrated that the proportion of iNKT cells (Vα14Jα18) increased within the heart at day 7 after α-GC administration and decreased at day 28 but remained higher than that in the sham group. In a model of experimental autoimmune encephalomyelitis, early immunization with α-GC protected against this disease, whereas later immunization potentiated it (41). In the present study, pretreatment with α-GC injection significantly enhanced iNKT cell infiltration,

and the most important finding was that the activation of iNKT cells (Vα14Jα18) by α-GC prior to MSC transplantation further attenuated LV remodeling after MI, which further improved the efficacy of MSCs on post-MI hearts compared with MSC transplantation. In 2009, Burchfield *et al.* (42) suggested that bone marrow mononuclear cells mediated cardiac protection (decreased T lymphocyte accumulation, reactive hypertrophy and myocardial collagen deposition) after MI, partly dependent on interleukin (IL)-10. In 2011, Dayan *et al.* (43) demonstrated that the mechanism of MSC-mediated enhancement of cardiac function possibly proceeded via an IL-10-mediated switch from infiltration of proinflammatory to anti-inflammatory macrophages at the infarct site. In addition, previous studies have indicated that the therapeutic effects of α-GC against TH1-like autoimmune diseases are mediated via a shift from a TH1 pattern toward a TH2 pattern and the induction of the immunosuppressive cytokine IL-10 (44, 45). Sobirin *et al.* (16) reported that iNKT cells have a protective role against post-MI remodeling and failure, partly through the enhanced expression of IL-10. In 2016, Tsutsui found that an anti-IL-10 receptor antibody abrogated the protective effects of α-GC on MI remodeling, suggesting that NKT cells play a protective role against post-MI LV remodeling and failure through the enhanced expression of cardioprotective cytokines such as IL-10 (46). It may be speculated that the potential mechanisms of iNKT cell activation after MSC transplantation against LV remodeling are partially mediated via enhanced expression of IL-10, a decrease in apoptotic cardiomyocytes, myocardial collagen deposition and LV failure; however, further study of the precise mechanism is required.

Of note, the present study has several limitations that must be acknowledged. First, previous studies have indicated the involvement of PGE_2, TGF-β1 and iNOS in various immunoregulatory activities of MSCs, and the present study only assessed these three factors, with the results indicating that TGF-β1 and iNOS do not have any involvement, whereas certain other molecules may be involved in the modulation of iNKT activities. Further study regarding this finding is required. Second, it is not possible to demonstrate the location of iNKT cells in postinfarct hearts *in situ* by immunohistochemical analysis or *in situ* hybridization. Further study of the realization of *in situ* detection is required to clarify this important issue.

Conclusion

The present study suggested that MSCs inhibited iNKT cell infiltration in post-MI mouse hearts, and activating iNKT cells enhanced the cardioprotective effect of MSCs and attenuated cardiac remodeling. Therapies designed to activate iNKT cells before MSC transplantation might be beneficial to enhance the effectiveness of MSCs in the post-MI heart. This approach may become a new direction of immune treatment for infarcted hearts.

Declarations

Ethics approval and consent to participate

No human studies were carried out by the authors for this article. Ethical approval for all work was received from the animal research committee of Zhengzhou University (Zhengzhou, China).

Consent for publication

Not applicable

Availability of data and materials

The data used to support the findings of this study are included within the article. If the additional data are needed, please contact the first author and corresponding authos.

Competing interests

The authors declare that there is no conflict of interest regarding the publication of this paper.

Fundings

No fundings was received for this study.

Authors' contributions

WT LI: Conceptualization, Methodology, Software; Y HUANG: Data curation, Writing- Original draft preparation; CY GAO: Supervision; ZY ZHU: Visualization, Investigation; GY DAI: Software, Validation, Methodology.

Acknowledgements

The authors wish to thank Dr XIAOJING SHI for the help and contributions to the infarcted mouse models and MSCs transplantation.

References

1. Ong S-B, Hernández-Reséndiz S, Crespo-Avilan GE, et al. Inflammation following acute myocardial infarction: Multiple players, dynamic roles, and novel therapeutic opportunities. J.pharmthera. 2018.01.001. Epub 2018 Jan 9.
2. L Kristin Newby. Inflammation as a Treatment Target after Acute Myocardial Infarction. N Engl J Med. 2019;381(26):2562–3.
3. Sumanth D, Prabhu, Nikolaos G, Frangogiannis. The Biological Basis for Cardiac Repair After Myocardial Infarction: From Inflammation to Fibrosis. Circ Res. 2016;119(1):91–112.
4. Van den Akker F, de Jager SC, Sluijter JP. Mesenchymal stem cell therapy for cardiac inflammation: immunomodulatory properties and the influence of toll-like receptors. Mediators Inflamm. 2013; 2013: 181020.
5. Alan J, Mouton OJ, Rivera ML, Lindsey. Myocardial infarction remodeling that progresses to heart failure: a signaling misunderstanding. Am J Physiol Heart Circ Physiol. 2018;315(1):H71–9.

6. Mikhail Konoplyannikov S, Kotova V, Baklaushev, et al. Mesenchymal Stem Cell Therapy for Ischemic Heart Disease: Advances and Challenges. Curr Pharm Des. 2018;24(26):3132–42.
7. Di Nicola M, Carlo-Stella C, Magni M, et al. Human bone marrow stromal cells suppress T-lymphocyte proliferation induced by cellular or nonspecific mitogenic stimuli. Blood. 2002;99(10):3838–43.
8. Prigione I, Benvenuto F, Bocca P, et al. Reciprocal interactions between human mesenchymal stem cells and gammadelta T cells or invariant natural killer T cells. Stem Cells. 2009;27(3):693–702.
9. Abumaree MH, Abomaray FM, Alshabibi MA, et al. Immunomodulatory properties of human placental mesenchymal stem/stromal cells. Placenta. 2017. pii: S0143-4004(17)30225-4.
10. Yufang Shi Yu, Wang Q, Li, et al. Immunoregulatory mechanisms of mesenchymal stem and stromal cells in inflammatory diseases. Nat Rev Nephrol. 2018;14(8):493–507.
11. Shobha Regmi S, Pathak JO, Kim, et al. Mesenchymal stem cell therapy for the treatment of inflammatory diseases: Challenges, opportunities, and future perspectives. Eur J Cell Biol. 2019;98(5–8):151.
12. Mengyuan Wang Q, Yuan L, Xie. Mesenchymal Stem Cell-Based Immunomodulation: Properties and Clinical Application. Stem Cells Int. 2018; 2018:3057624.
13. Catherine M, Crosby M. Kronenberg. Tissue-specific functions of invariant natural killer T cells. Nat Rev Immunol. 2018;18(9):559–74.
14. Gazdic M, Simovic Markovic B, Vucicevic L, et al. Mesenchymal stem cells protect from acute liver injury by attenuating hepatotoxicity of liver natural killer T cells in an inducible nitric oxide synthase- and indoleamine 2,3-dioxygenase-dependent manner. J Tissue Eng Regen Med. 2017. doi:10.1002/term.2452.
15. Chiara Rizzo LL, Barbera ML, Pizzo, et al. Invariant NKT Cells and Rheumatic Disease: Focus on Primary Sjogren Syndrome. Int J Mol Sci. 2019;20(21):5435.
16. Sobirin MA, Kinugawa S, Takahashi M, et al. Activation of natural killer T cells ameliorates postinfarct cardiac remodeling and failure in mice. Circ Res. 2012;111(8):1037–47.
17. Tsuneaki H, Shintaro K, Masashige T, et al. Activation of invariant natural killer T cells by α-galactosylceramide ameliorates myocardial ischemia/reperfusion injury in mice. J Mol Cell Cardiol. 2013;62:179–88.
18. Kawano T, Cui J, Koezuka Y, et al. CD1d-restricted and TCR-mediated activation of valpha14 NKT cells by glycosylceramides. Science. 1997;278:1626–9.
19. Salto-Tellez M, Yung Lim S, El-Oakley RM, et al. Myocardial infarction in the C57BL/6J mouse: a quantifiable and highly reproducible experimental model. Cardiovasc Pathol. 2004;13(2):91–7.
20. Karpov AA, Uspenskaya YK, Minasian SM, et al. The effect of bone marrow- and adipose tissue-derived mesenchymal stem cell transplantation on myocardial remodeling in the rat model of ischaemic heart failure. Int J Exp Pathol. 2013;94(3):169–77.
21. Eguchi T, Kumagai K, Kobayashi H, et al. Accumulation of invariant NKT cells into inflamed skin in a novel murine model of nickel allergy. Cell Immunol. 2013; 284(1–2): 163 – 71.

22. Israel M, Barbash P, Chouraqui J, Baron, et al. Systemic delivery of bone marrow-derived mesenchymal stem cells to the infarcted myocardium: feasibility, cell migration, and body distribution. Circulation. 2003;108(7):863–8.
23. Atsushi Anzai T, Anzai S, Nagai, et al. Regulatory role of dendritic cells in postinfarction healing and left ventricular remodeling. Circulation. 2012;125:1234–45.
24. Sarah A, Dick JA, Macklin S, Nejat, et al. Self-renewing resident cardiac macrophages limit adverse remodeling following myocardial infarction. Nat Immunol. 2019;20(1):29–39.
25. Kyle I, Mentkowski LM, Euscher A, Patel, et al. Monocyte recruitment and fate specification after myocardial infarction. Am J Physiol Cell Physiol. 2020;319(5):C797–806.
26. Arslan F, de Kleijn DP, Pasterkamp G. Innate immune signaling in cardiac ischemia. Nat Rev Cardiol. 2011;8:292–300.
27. Ehsan Vafadarnejad G, Rizzo L, Krampert, et al. Dynamics of Cardiac Neutrophil Diversity in Murine Myocardial Infarction. Circ Res. 2020;127(9):e232–49.
28. Frangogiannis NG. Regulation of the inflammatory response in cardiac repair. Circ Res. 2012;110:159–73.
29. Dong F, Khalil M, Kiedrowski M, et al. Critical role for leukocyte hypoxia inducible factor-1alpha expression in post-myocardial infarction left ventricular remodeling. Circ Res. 2010;106(3):601–10.
30. Kobara M, Noda K, Kitamura M, et al. Antibody against interleukin-6 receptor attenuates left ventricular remodelling after myocardial infarction in mice. Cardiovasc Res. 2010;87(3):424–30.
31. Poggi A, Maria R, Zocchi. Immunomodulatory Properties of Mesenchymal Stromal Cells: Still Unresolved "Yin and Yang". Curr Stem Cell Res Ther. 2019;14(4):344–50.
32. María Del Pilar De la Rosa-Ruiz, Marco Antonio Álvarez-Pérez, Víctor Adrián Cortés-Morales, et al. Mesenchymal Stem/Stromal Cells Derived from Dental Tissues: A Comparative In Vitro Evaluation of Their Immunoregulatory Properties Against T cells. Cells. 2019; 8(12):1491.
33. Campos-Mora CTerraza-Aguirre,M, Elizondo-Vega R, et al. Mechanisms behind the Immunoregulatory Dialogue between Mesenchymal Stem Cells and Th17 Cells. Cells. 2020;9(7):1660.
34. Séverine Loisel J. Dulong, Cédric Ménard, et al. Brief Report: Proteasomal Indoleamine 2,3-Dioxygenase Degradation Reduces the Immunosuppressive Potential of Clinical Grade-Mesenchymal Stromal Cells Undergoing Replicative Senescence. Stem Cells. 2017;35(5):1431–6.
35. Van Kaer L. α-Galactosylceramide therapy for autoimmune diseases: prospects and obstacles. Nat Rev Immunol. 2005;5:31–42.
36. Wilson MT, Johansson C, Olivares-Villagómez D, et al. The response of natural killer T cells to glycolipid antigens is characterized by surface receptor down-modulation and expansion. Proc Natl Acad Sci U S A. 2003;100:10913–8.
37. Crowe NY, Uldrich AP, Kyparissoudis K, et al. Glycolipid antigen drives rapid expansion and sustained cytokine production by NK T cells. J Immunol. 2003;171:4020–7.

38. Li L, Huang L, Vergis AL, et al. IL-17 produced by neutrophils regulates IFN-gamma-mediated neutrophil migration in mouse kidney ischemia–reperfusion injury. J Clin Invest. 2010;120:331–42.
39. Cao Z, Yuan Y, Jeyabalan G, et al. Preactivation of NKT cells with alpha-GalCer protects against hepatic ischemia–reperfusion injury in mouse by a mechanism involving IL-13 and adenosine A2A receptor. Am J Physiol Gastrointest Liver Physiol. 2009;297:G249–58.
40. Tetsuji Aoyagi N, Yamamoto M, Hatta, et al. Activation of pulmonary invariant NKT cells leads to exacerbation of acute lung injury caused by LPS through local production of IFN-gamma and TNF-alpha by Gr-1 + monocytes. Int Immunol. 2011;23:97–108.
41. Jahng AW, Maricic I, Pedersen B, et al. Activation of natural killer T cells potentiates or prevents experimental autoimmune encephalomyelitis. J Exp Med. 2001;194:1789–99.
42. Burchfield JS, Iwasaki M, Koyanagi M, et al. Interleukin-10 from transplanted bone marrow mononuclear cells contributes to cardiac protection after myocardial infarction. Circ Res. 2008;103(2):203–11.
43. Dayan V, Yannarelli G, Billia F, et al. Mesenchymal stromal cells mediate a switch to alternatively activated monocytes/macrophages after acute myocardial infarction. Basic Res Cardiol. 2011;106(6):1299–310.
44. Hong S, Wilson MT, Serizawa I, et al. The natural killer T-cell ligand alpha-galactosylceramide prevents autoimmune diabetes in non-obese diabetic mice. Nat Med. 2001;7:1052–6.
45. Chen D, Liu H, Wang Y, et al. Study of the adoptive immunotherapy on rheumatoid arthritis with Thymus-derived invariant natural killer T cells. Int Immunopharmacol. 2019;67:427–40.
46. Hiroyuki Tsutsui. Role of natural killer T cells in cardiac remodeling and failure and the development of novel therapeutic strategy. Fukuoka Igaku Zasshi. 2016;107(10):177–84.

Figures

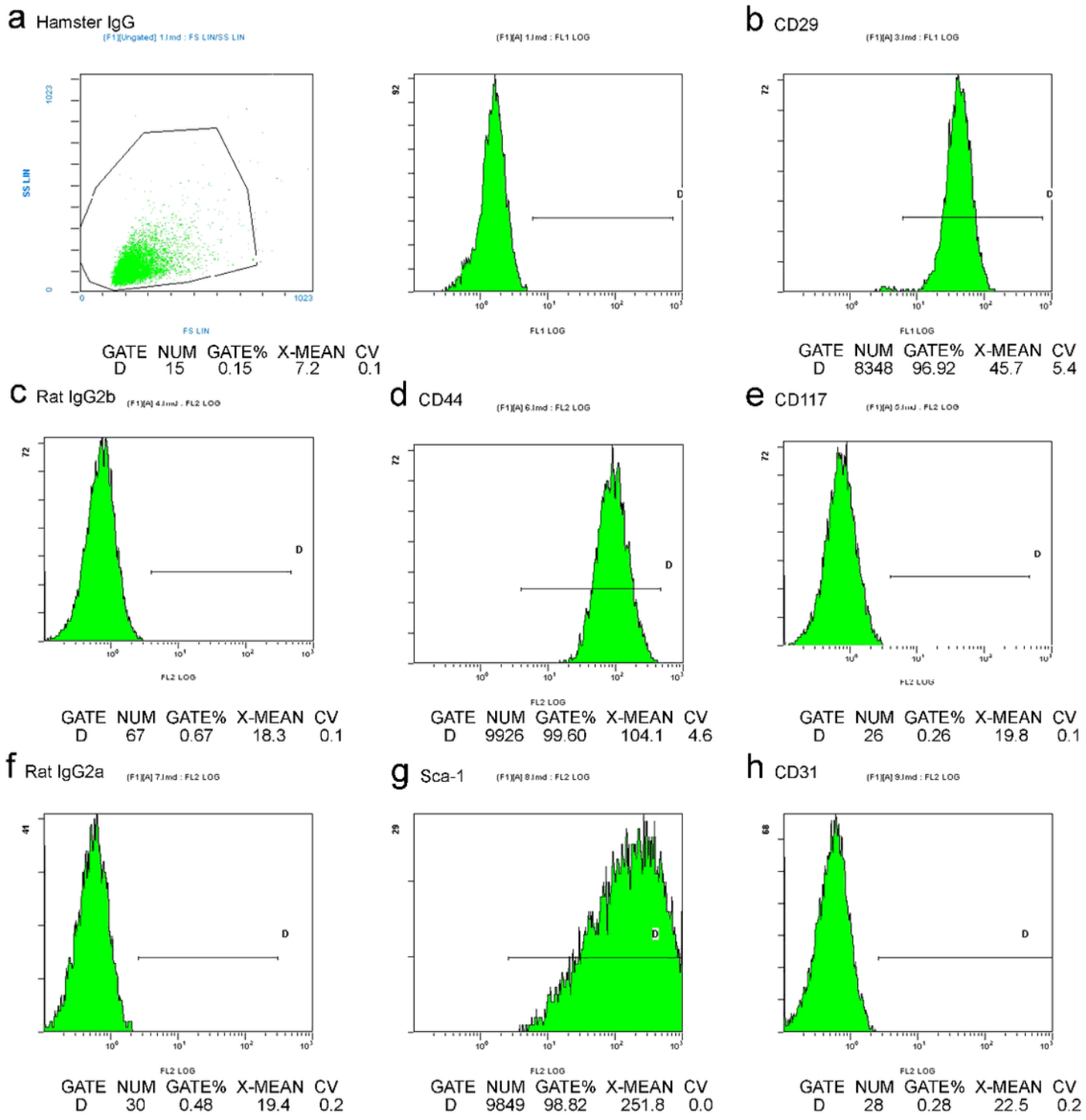

Figure 1

The cell surface phenotypes (CD29+, CD44+, Sca-1+, CD117- and CD31-) characterized by fluorescence-activated cell sorting analysis were performed.

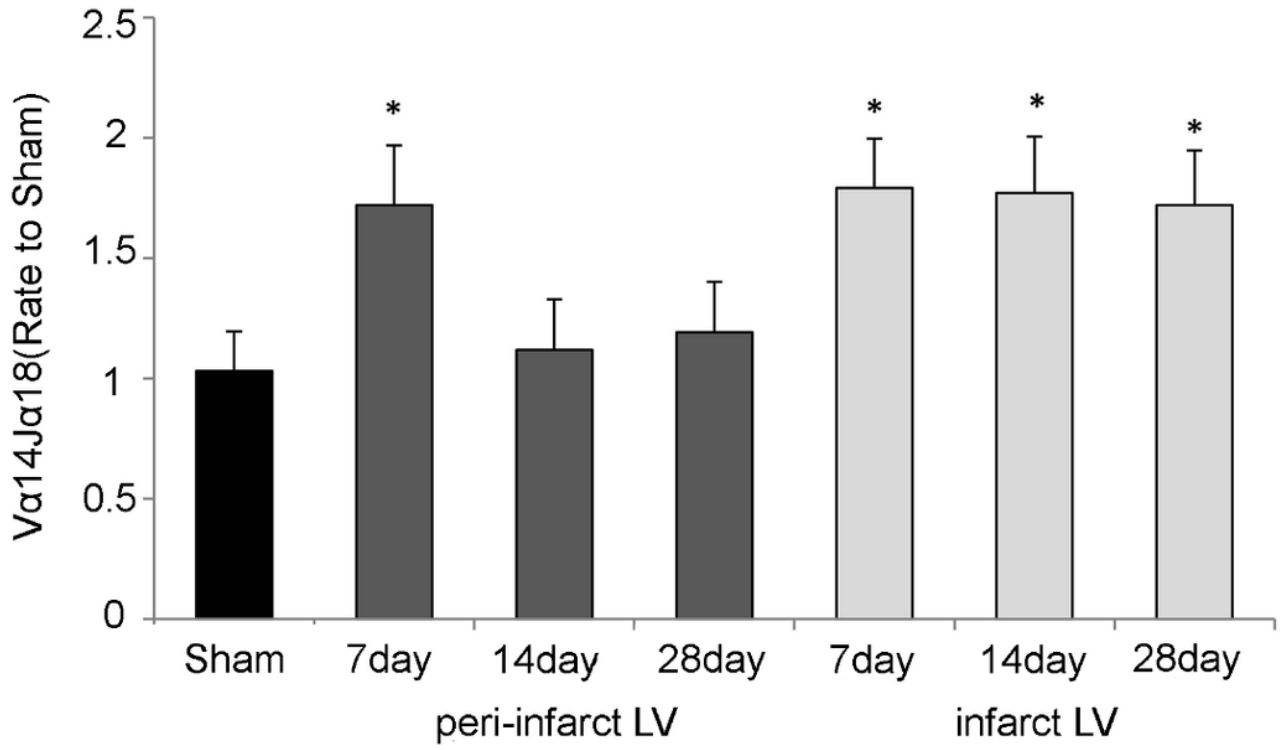

Figure 2

Gene expression of Vα14Jα18 in infarct and peri-infarct LVs after surgery. The figures are expressed as the ratio to Sham values. Data are expressed as the mean±SD. *P<0.05 vs Sham. LV: left ventricular

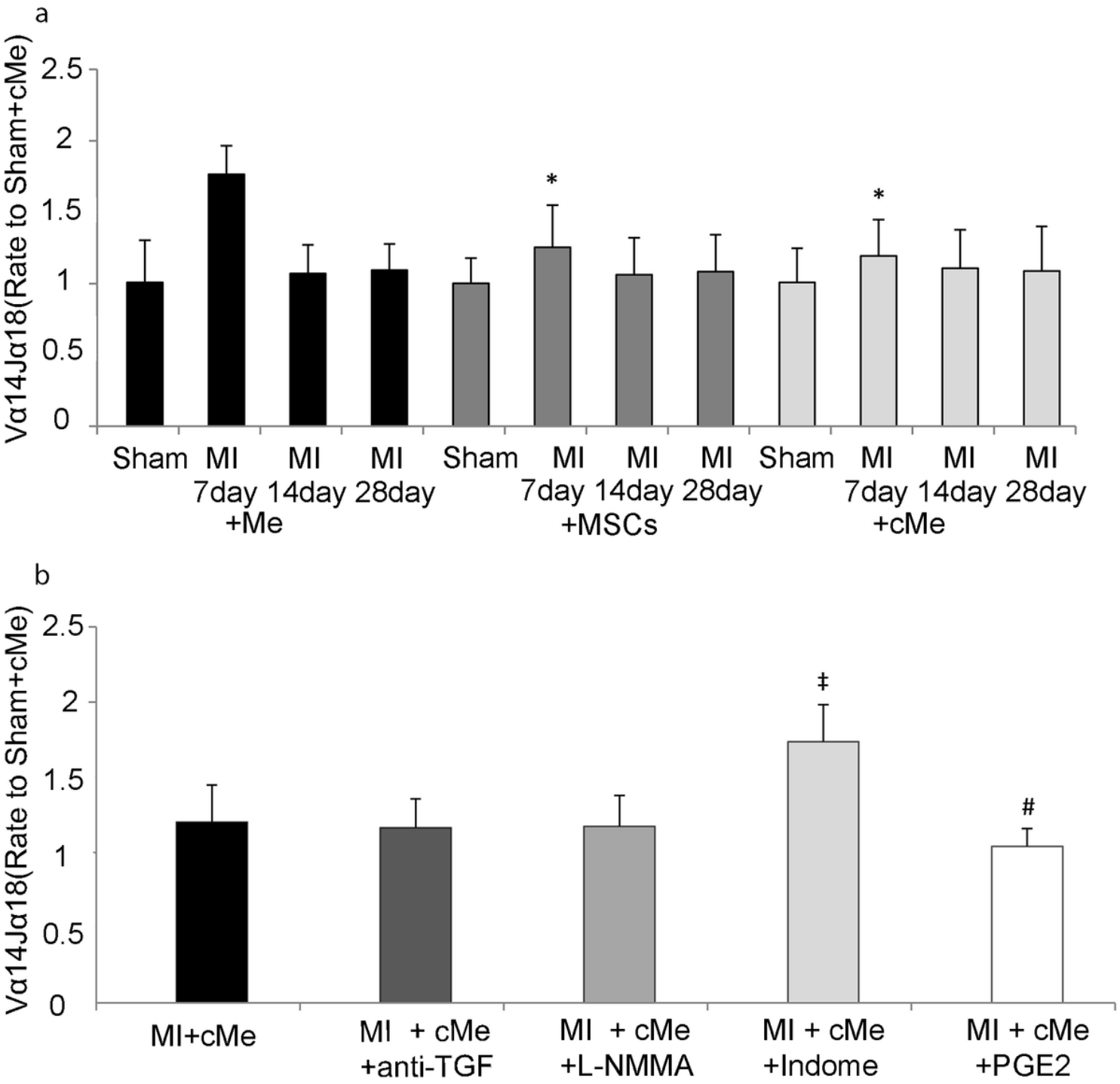

Figure 3

a. Gene expression of Vα14Jα18 in peri-infarct LV with the injection of serum-free medium，complete medium，and complete medium+MSCs after surgery at day 7, 14, and 28．b. Gene expression of Vα14Jα18 in peri-infarct LVs injected with PGE2, L-NMMA, indome and anti-TGF at day 7. The figures are expressed as the ratio to Sham+cMe values. Data are expressed as the mean±SD. Me: serum-free medium, cMe: complete medium. *P<0.05 vs MI+Me at day 7; ‡P<0.05 vs MI+cMe; #P<0.05 vs MI+cMe+Indome.

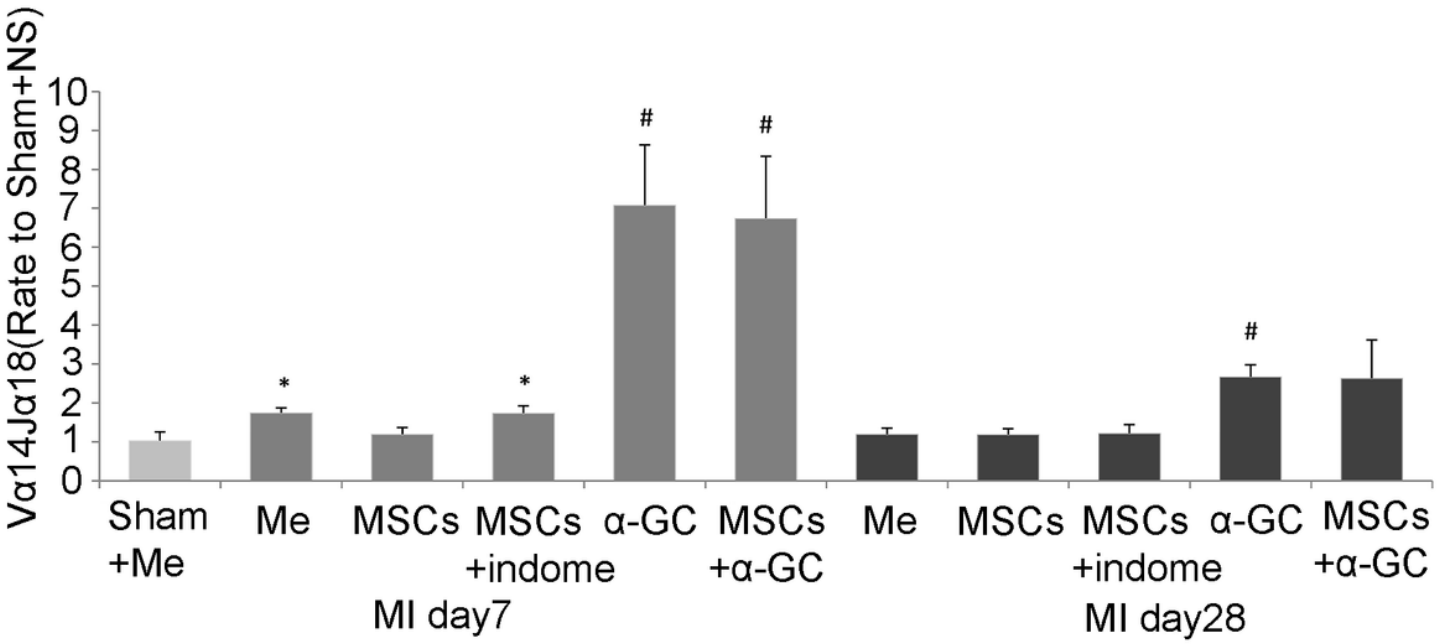

Figure 4

Gene expression of Vα14Jα18 in peri-infarct LVs with the injection of Me, MSCs, and α-GC after surgery at days 7 and 28. *P<0.05 vs MI+MSCs at day 7; #P<0.05 vs MSCs. There was no significant difference between the MI+α-GC and MI+MSCs+α-GC groups at days 7 and 28.

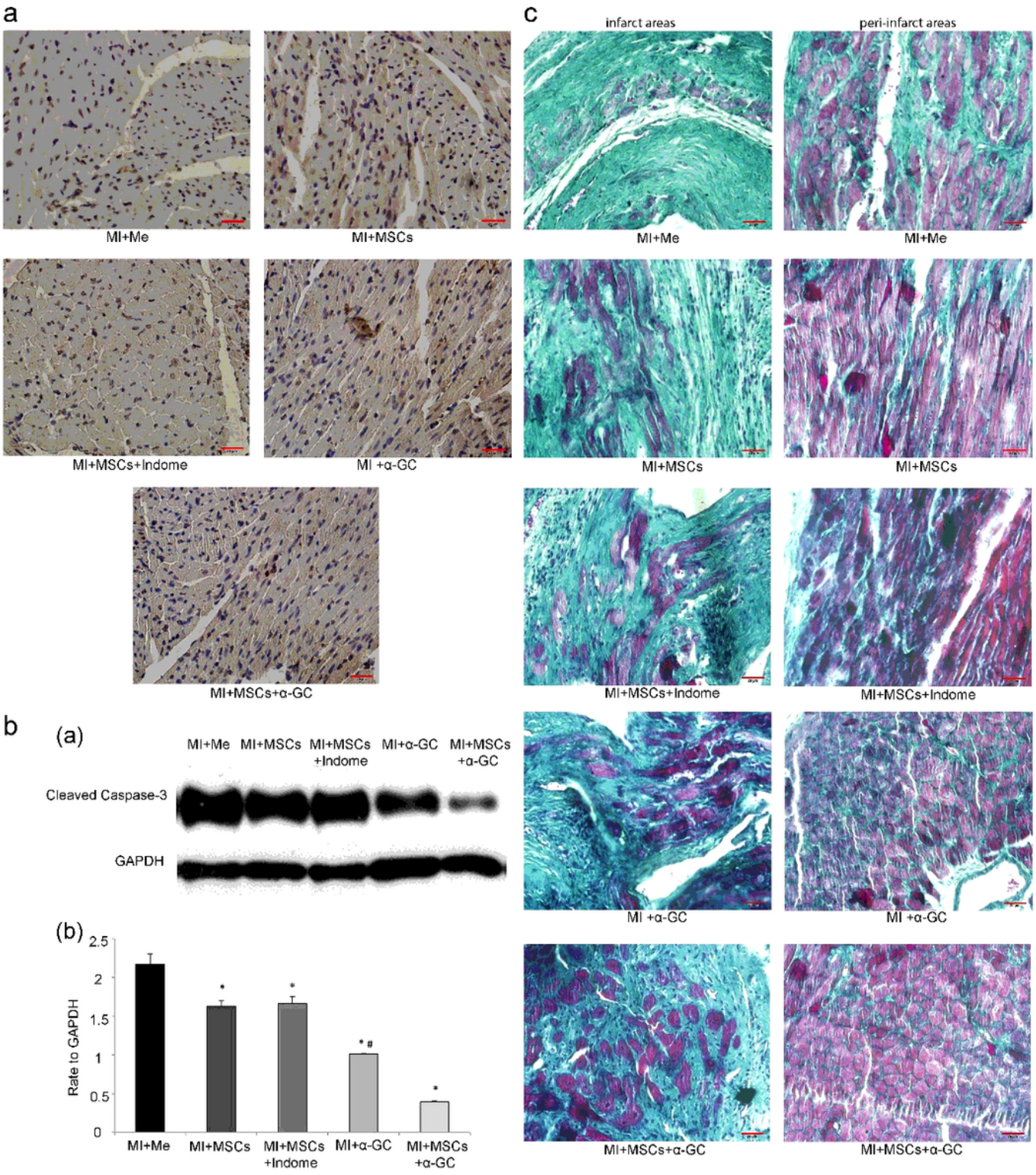

Figure 5

a. Representative photomicrographs of TUNEL staining of LV sections from MI+Me, MI+MSCs, MI+MSCs+indome, MI+α-GC and MI+MSCs+α-GC groups in the peri-infarct area. Scale bar, 20 μm. b. Representative immunoblotting analysis and histogram of gray values for Caspase-3/GAPDH. Data are expressed as the mean±SEM, *P□0.05 vs MI+Me, #P□0.05 versus MI+MSCs+α-GC. c. Representative high-power photomicrographs of LV cross sections stained with Masson trichrome from MI+Me, MI+MSCs,

MI+MSCs+indome, MI+α-GC and MI+MSCs+α-GC groups in infarct and peri-infarct areas. Scale bar, 20 μm.

Supplementary Files

This is a list of supplementary files associated with this preprint. Click to download.

- AuthorChecklistE10only.pdf
- uncroppedblotsimages.docx